Single molecule measurements within individual membrane-bound ion channels using a polymer-based bilayer lipid membrane chip†‡

Louis P. Hromada,[a] Brian J. Nablo,[b] John J. Kasianowicz,[b] Michael A. Gaitan[b] and Don L. DeVoe*[a]

The measurement of single poly(ethylene glycol) (PEG) molecules interacting with individual bilayer lipid membrane-bound ion channels is presented. Measurements were performed within a polymer microfluidic system including an open-well bilayer lipid membrane formation site, integrated Ag/AgCl reference electrodes for on-chip electrical measurements, and multiple microchannels for independent ion channel and analyte delivery. Details of chip fabrication, bilayer membrane formation, and α-hemolysin ion channel incorporation are discussed, and measurements of interactions between the membrane-bound ion channels and single PEG molecules are presented.

Introduction

Synthetic Bilayer Lipid Membranes (BLMs) have been widely used to perform electrophysiological analyses of membrane proteins following the seminal BLM reconstitution work of Mueller and coworkers in the early 1960s.[1–3] The mechanics of membrane formation have been extensively studied,[4–8] together with the incorporation of membrane proteins, such as ion channels, into BLMs.[9–11] Ion channels integrated into BLMs have been used to detect a variety of atomic and molecular species. For example, α-hemolysin (α-HL) ion channels incorporated into synthetic BLMs have been employed to detect H^{+},[12] ssDNA,[13] dextran,[14] poly(vinyl pyrrolidone),[14] and Na poly(styrene sulfonate)[15] as these analytes occlude and possibly translocate through the channels′ lumen.

While there has been substantial progress in ion channel research, experimental platforms used for BLM formation and ion channel measurements have remained essentially unchanged. Typically, BLMs are formed across an aperture fabricated in hydrophobic polytetrafluoroethylene (PTFE) film, which separates two chambers each containing aqueous salt solution and an electrode to monitor trans-membrane currents.[5,16,17] These large-scale platforms suffer from several limitations, such as large perfusion times when removing unwanted reagents, high stray capacitances which limit the bandwidth of electrophysiological measurements, and limited data throughput due to single-site

[a]University of Maryland, College Park, Department of Mechanical Engineering, College Park, Maryland, 20742, USA.
E-mail: ddev@umd.edu; Fax: +1-301-314-9477; Tel: +1-301-405-8125
[b]National Institute of Standards and Technology, Electronics and Electrical Engineering Laboratory, Gaithersburg, Maryland, 20899, USA

† Certain commercial materials and equipment are identified in order to specify adequate experimental procedures. In no case does such identification imply recommendation or endorsement by the National Institute of Standards and Technology, nor does it imply that the items identified are necessarily the best available for the purpose.
‡ The HTML version of this article has been enhanced with colour images.

measurements. Furthermore, these benchtop systems are not suitable for field-deployable biosensing applications.

Recently, the development of microfluidic systems as BLM platforms has been investigated. Early work in this area employed quartz,[18,19] Si/glass,[20,21] and Si/SiN[22] materials, with bulk micromachining techniques used in the latter cases to create microchannels on opposing Si wafer sides together with enclosed apertures connecting the channels. Because silicon's semiconducting nature resulted in high parasitic capacitance and unwanted noise, polymer-based microfluidic devices were later investigated. Polymer devices also offer potential benefits for low cost chip fabrication for disposable biosensor applications. Suzuki et al. first reported the development of polymer BLM chips using poly(methyl methacrylate) (PMMA) substrates patterned by CNC machining, with a mechanically-milled open conical well and aperture to support BLM formation.[23] A similar PMMA chip was later demonstrated with multiple BLM sites in a single reservoir.[24] A related device was developed with in situ BLM formation achieved by thinning a lipid plug to produce two contacting monolayers.[25,26] Sandison et al. have also described the development of polymer BLM chips fabricated from PMMA,[27,28] and PTFE/glass.[29] Incorporation of alamethicin,[23] gramicidin,[30] α-HL,[31] and Methanobacterium Thermoautotrophicum K^{+} (MthK)[32] ion channels have been reported in these various polymer devices.

Here, we report the measurement of single analyte molecules interacting with membrane-bound ion channels in a polymer microfluidic BLM platform. The integrated sensor platform is fabricated from polycarbonate (PC) as the primary substrate with BLM formation occuring on a polyvinylidene chloride (PVDC) supporting layer, which is historically capable of sustaining BLMs.[4,7] The access well chip design employs a two-layer channel network capable of independently delivering ion channels and analyte molecules to the BLM sensing site.

A common feature of reported polymer BLM devices is the use of bulk Ag/AgCl electrode wires for electrical interrogation, with the majority of these platforms employing wires inserted into reservoirs or fluid compartments within the chips.[23–32] In a

step towards further integration, a device consisting of multiple elastomeric polydimethylsiloxane (PDMS) layers developed by Malmstadt et al.[33,34] employs Ag/AgCl electrode wires cast directly into the PDMS layers.[34] Regardless of the approach, the use of bulk electrodes requires relatively large distances between the wires and BLM sensing sites, necessitating large microchannels to minimize series resistance to the BLM site. Following the previous approach of Ogier et al.[35,36] and Wilk et al.,[37] the present work uses lithographically patterned thin film Ag/AgCl electrodes capable of monitoring BLM formation, ion channel incorporation, and interactions between the ion channels and analyte molecules. By placing the electrodes close to the BLM site, smaller microchannels can be used without unduly increasing series resistance and sacrificing sensor bandwidth.

Operation of the integrated platform is demonstrated, with BLM formation achieved by manually painting lipid through an open reservoir. Unlike previous open-well chips in which lipid bilayers were formed by exposing the BLM aperture to air to encourage thinning of the lipid solution,[24,38,39] here the bilayers were created by directly painting the apertures with small volumes of lipid using a glass brush. Unlike previous work employing lipid painting for BLM formation in microfluidic systems,[40] the method reported here utilizes a low miscible water phase solvent as the lipid carrier. This technique eases the requirement of precise volumetric control typically when using the painting method, since excess lipid carrier removed by diffusion into the water phase will result in lipid thinning as required for efficient BLM formation.

Using this platform, incorporation of single α-HL ion channels into the lipid membranes is demonstrated by introducing the protein through an integrated microchannel. In the following, the detection and characterization of single poly(ethylene glycol) (PEG) molecules interacting with the membrane-bound α-HL ion channels is described.

Materials and methods

BLM chip fabrication

The primary structure of the integrated BLM chip consists of an upper and lower PC wafer bonded on either side of a thin PVDC film, with Ag/AgCl electrodes deposited on the upper surface of the PVDC layer. A plan and section view illustrating an open-faced BLM chip is shown in Fig. 1. The fabrication sequence starts with 8.9 cm diameter top and bottom PC wafers machined from 2.38 mm thick sheets (Sheffield Plastics, Sheffield, MA). The polymer wafers are patterned by hot embossing directly from SU-8 photoresist (Microchem, Newton, MA) features photopatterned on 10 cm diameter silicon wafers. Open microchannels, nominally 60 μm wide and 50 μm deep, were formed in the top and bottom PC wafers using an optimized imprinting protocol. After imprinting, a series of 700 μm diameter holes are drilled in the top PC wafer at the end of each microchannel. The access well is then formed using a 3 mm diameter × 2.2 mm deep countersink drill with a 130° tip angle. Holes to receive electrode terminals are also drilled and tapped.
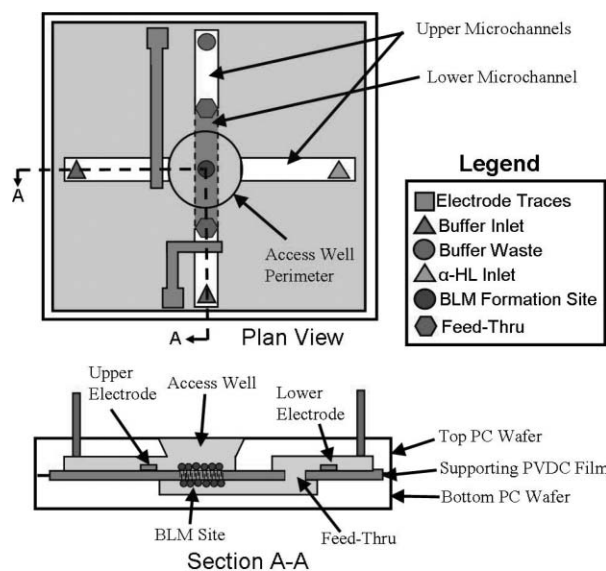
Fig. 1 Plan and section of an open-faced BLM chip with integrated Ag/AgCl electrodes. The multilayer chip is approximately 5 cm square.

A 12.5 μm thick PVDC film (Filcon, Clare, MI) is applied to the entire surface of the bottom PC wafer, enclosing the imprinted microchannels in that layer. The PVDC film is used as the supporting layer for BLM formation, while also serving as a thermal bonding layer between the PC wafers for sealing the upper and lower microchannels. The film also serves as a substrate for Ag/AgCl electrode fabrication. After applying the PVDC film, small holes with diameters of approximately 20–40 μm are burned into the PVDC film using a hot needle[3–5,41] with hole alignment achieved by mounting the needle on the mobile base of a probe station equipped with steroscopic optics. One of these holes is used as the BLM formation site, while the remaining holes serve as feedthroughs between the upper and lower microchannels. An electron micrograph of a typical BLM formation hole is shown in Fig. 2. Thin film Ag/AgCl electrodes are then defined on the PVDC film. A 175 μm thick brass shadowmask was first aligned to the bottom PC wafer. Adapting a process described by Polk and coworkers,[42] sequential layers of Cr, Au, and Ag were thermally evaporated with thickness of 10, 10, and 100 nm, respectively. An electroplating process was then used to increase the Ag film thickness, thereby improving electrode stability and reducing the likelihood of thermal cracks developing during the chip bond cycle. Electroplating was
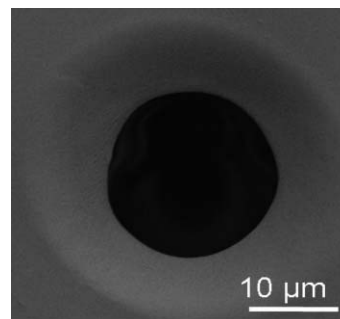
Fig. 2 Electron micrograph of a ~20 μm diameter BLM formation hole fabricated in a PVDC film using a hot needle.

performed by pooling ~700 μL of plating solution (350 mM AgNO₃ in 1 M NH₃) with a Pt counter electrode submerged in the plating solution. Each electrode was plated individually by applying a current of 16 mA (0.33 mA/mm²) for 35 seconds. The exposed Ag trace tips were then chloridized by pipetting ~3 μL of 350 mM ferric chloride aqueous solution and waiting 1 min before a final DI water rinse and N₂ blow dry.

After electrode fabrication is complete, the top and bottom PC wafers are aligned and placed in a hot press (AutoFour/15, Carver, IA) and thermally bonded at 141 °C under a pressure of 280 psi for approximately 10 minutes. After dicing the bonded chip, hypodermic needle tubing (22s gauge, Hamilton, Reno, UT) sections are inserted into the 700 μm diameter holes previously drilled through the upper PC wafer, creating a low dead-volume, high-pressure fluidic interface to off-chip capillary connections. Finally, electrical connections to the Ag/AgCl electrodes were completed by inserting brass screws into the tapped holes aligned to the electrode ends. To form reliable and low-noise contacts, the tapped holes were initially packed with Ag-filled grease prior to inserting the brass screw. A completed chip is shown in Fig. 3(a), with an overhead view of the access well and top electrode in Fig. 3(b). Fig. 3(c) reveals the BLM formation site, approximately 50 μm in diameter, aligned with the lower microchannel. The fabricated device was found to have a parasitic capacitance of 6.4 pF, and a series resistance of 214 kΩ when filled with a 1 M NaCl solution.

Experimental setup

The BLM chips were tested on an Axiovert 200 microscope equipped with an Axiocam MRm camera (Carl Zeiss Inc., NY) for video capture. Syringe pumps (PHD 2000, Harvard Apparatus, Holliston, MA) used for fluid delivery are connected to a DAQ-enabled computer for remote control. The entire test setup was positioned within a Faraday cage, which was located on a vibration isolation table to minimize external noise.

An Axopatch 200B amplifier (Molecular Devices, CA) with a high impedance headstage was used to apply input membrane voltage-clamping potentials to the on-chip Ag/AgCl electrodes and to convert measured membrane current to a proportional output voltage. Positive potentials drive cations from the access well to the lower microchannel. The output signal was filtered using a 4-pole Bessel filter ($f_c = 10$ kHz) onboard the amplifier prior to being digitized by a Digidata 1440A (Molecular Devices, Sunnyvale, CA) at a 50 kHz sampling rate. All electrical signals (voltage input and current output) were recorded digitally using Clampex 10 software (Molecular Devices, Sunnyvale, CA), with all signals displayed together with syringe pump conditions and microscope video in real-time using custom software.

BLM Formation

The painted BLMs are formed from a 9 : 1 v/v n-hexanol : n-hexadecane mixture containing 15 mg/ml diphytanoyl phospatidylcholine (1,2-diphytanoyl-sn-glycero-3-phosphocholine; Avanti Lipids, AL). No pretreatment of the PVDC surface surrounding the BLM formation hole was utilized, however the hole was cleaned with n-pentane multiple times and allowed to evaporate prior to testing. An aqueous buffer solution consisting of 1 M NaCl and 5 mM 2-morpholinoethanesulfonic acid monohydrate (MES, pH 7, 80 mS/cm) was used unless otherwise specified.

After filling the entire chip with buffer, lipid solution was delivered to the BLM formation site using a custom-fabricated glass (Pyrex) brush. The glass brush has one end thermally drawn down to a fire-polished ball approximately 300 μm in diameter. The ball was rolled sparingly in the lipid solution, submerged into the access well until the ball end touched the PVDC film. The ball was gently slid across the BLM formation site before being lifted off the PVDC film and removed from the access well. In cases where painting failed to produce a BLM, the glass brush was cleaned with n-pentane and dried prior to repeating the formation process. The BLM diameter was estimated optically using a calibrated graded microscope reticule.

α-HL Ion channel incorporation

Ion channel solution was prepared by reconstituting α-HL in 10 mM Sodium Phosphate (LIST Biological Laboratories, Cambell, CA) at pH 7.2. The solution was delivered to the BLM site by either pipetting into the access well, or by injection through the upper or lower microchannels. For multiple ion channel incorporation, 500 μg/mL α-HL solution was injected using a syringe pump through the top microchannel at a flow rate of 15 μL/h. The injection was halted as soon as conductance jumps were observed in the current. For single ion channel incorporation, a 1.5 μL volume of 50 μg/mL α-HL solution was directly pipetted into the access well.

PEG Detection

Prior to BLM formation and α-HL channel incorporation, the lower microchannel was filled with a 50 μM PEG containing buffer solution. The PEG solution was prepared using polydisperse PEG with an average MW of 1500 g/mol (Fluka,
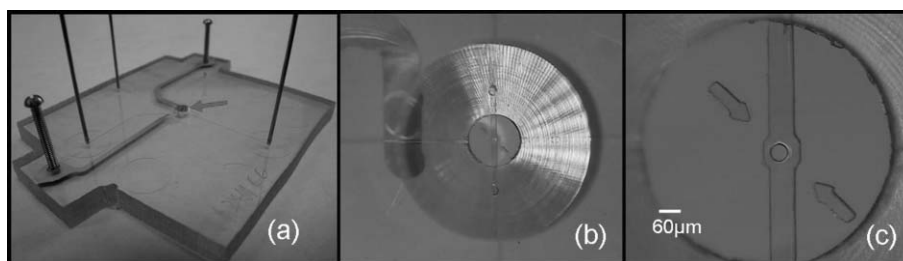
Fig. 3 (a) An open-faced BLM chip with arrow indicating location of access well containing the BLM formation site. (b) Overhead view of 3 mm diameter access well, with upper Ag/AgCl electrode shown. (c) Detail of BLM formation site (~45 μm in diameter) and lower microchannel.

Aldrich) in 3 M KCl and 10 mM MES at pH 7.05. After BLM formation and α-HL channel incorporation, PEG blockades occur spontaneously. These blockades are produced when PEG molecules occlude the α-HL lumen thus temporarily altering the measured ionic current.

Raw current signals were analyzed offline using *MATLAB* software to identify and characterize the single state PEG blockades. The *MATLAB* program generates histograms displaying relative frequencies of average blockade currents and blockade lifetimes. In constructing the histograms, a 5σ noise floor is computed assuming that the open channel current has a normal distribution. PEG blockades are defined by events in which the current drops below the noise floor for a minimum set of consecutive data points (typically > 5), which is set by the current sampling and filtering frequency. For instance, blockades lasting 100 μs (f_c = 10 kHz) must contain 5 data points (f_s = 50 kHz), with shorter blockades considered noise. For each blockade event, the mean and standard deviation of the current is computed and then the blockade lifetime is calculated by the absolute time difference between the first and last blockade data point within the blockade noise envelope.

Results and discussion

Fig. 4 shows a series of still frames acquired from an experimental video taken during BLM formation. The 20 mV$_{p-p}$ 250 Hz triangular input voltage waveform and output current waveform are shown for each frame. The first frame (a) shows the submerged glass brush painting lipid solution across the BLM formation site. As the brush is moved across the BLM formation site, the current output transitions from a saturated triangular waveform to a hybrid waveform as the brush occludes the hole. Frame (b) shows the BLM formation site immediately after successful application of lipid solution to the hole. The hybrid output waveform begins to transform as the hexanol diffuses away from the BLM site into the surrounding buffer. Frame (c) shows the still-changing output waveform seconds later. Finally, a stable squarewave current output can be seen in frame (d) indicative of capacitive coupling across the BLM formation site, indicating that the BLM has successfully formed. In this example, the final current output is 400 pA$_{p-p}$. The

final membrane appeared similar to previously reported BLM images,[38] with a diameter optically measured at approximately 40 μm. After subtracting stray chip capacitance, the BLM specific capacitance was determined to be 0.8 μF/cm^2.

Multiple α-HL channel incorporation

Following α-HL injection, multiple conductance jumps above the nominal current level typically occurred within 15 minutes, as shown in Fig. 5, due to incorporation of the ion channels into the BLM. Three of the four conductance jumps shown in this figure are approximately 40 pA in magnitude, which is reasonable given the applied DC voltage and salt concentration used. The atypical third conductance jump, shown in Fig. 5, is likely the result from differing channel conformation or occlusion.[43]
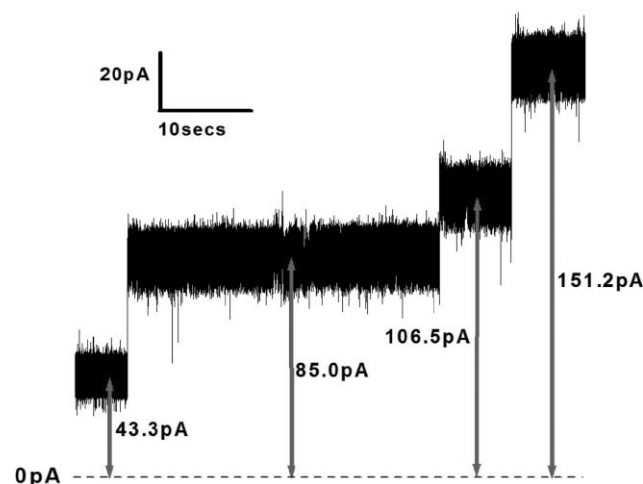
Fig. 5 Current output showing four distinct α-HL conductance jumps, with average current values at each step, using 1 M NaCl buffer. Data filtered with an 8-pole Bessel low pass filter (f_c = 1 kHz) with the applied voltage clamped at 40 mV.

Successful α-HL channel incorporation can be verified by studying the current–voltage (I–V) relationship. α-HL channels exhibit a non-linear, rectifying I–V relationship[43,44] where the degree of rectification can be determined by comparing the ratio of current magnitudes at equivalent positive and negative
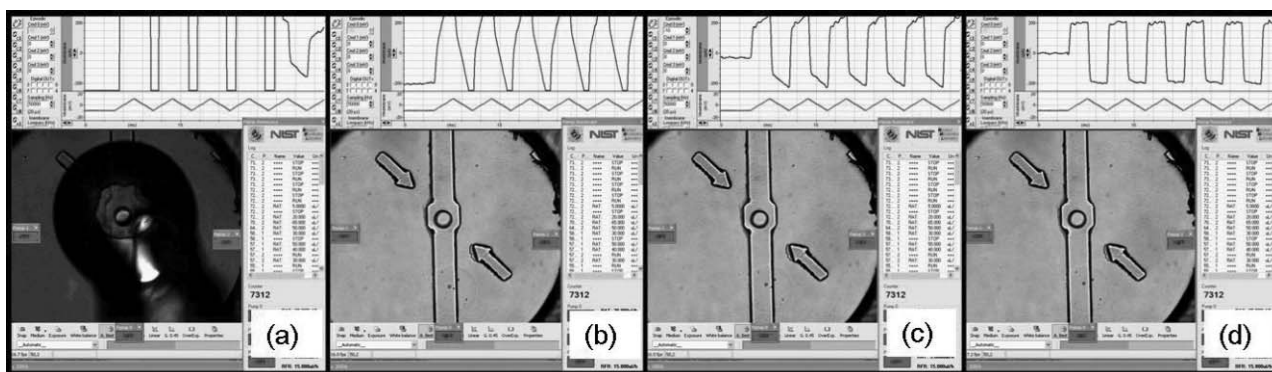
Fig. 4 Sequential images showing the BLM formation process. (a) Glass brush painting lipid solution over the BLM formation site. Note, output current waveform (upper trace) is saturated prior to brush occluding hole. Input clamping waveform is 20 mVp-p, 250 Hz triangle (lower trace). (b) Output current waveform immediately after brush removal. (c) As alcohol diffuses away, current waveform reducing to a squarewave, and (d) after 10 seconds, squarewave is stable indicating BLM is formed.

potentials, *e.g.* |I(V_{-120mV})/I(V_{120mV})|. The I–V curve plotted in Fig. 6 was constructed from four averaged I–V runs taken from the α-HL channel experiment described in Fig. 5. Using a known value of ~1 pA/mV for the specific conductance of a single full state α-HL channel in 1M NaCl buffer, the slope of the I–V curve presented in Fig. 6 reveals 4.5 channels inserted into the BLM during this experiment. Increased error at greater potentials is due to individual α-HL channels gating during data collection. The I–V data is qualitatively similar to data reported for a single α-HL channel under nearly identical test conditions.[43]
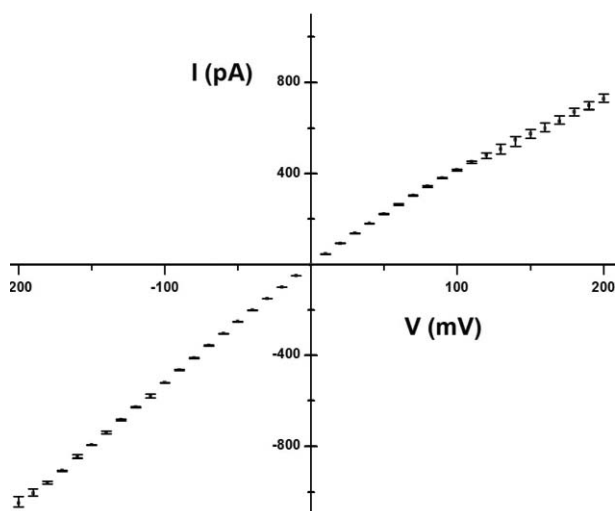
Fig. 6 Averaged current–voltage response for multiple α-HL channels incorporated in BLM shown in Fig. 5 using 1 M NaCl buffer.

Poly(ethylene glycol) detection

When PEG-1500 was introduced into a microchannel, PEG-induced blockades were immediately seen upon incorporation of a single α-HL channel. A current trace revealing a sequence of blockades measured using a BLM chip with an open channel current of ~140 pA is shown in Fig. 7(a). Unlike the data presented in Fig. 5 and 6, which were collected using a 1 M NaCl buffer, the blockade data presented in Fig. 7 were collected using a 3 M KCl buffer, resulting in a different specific conductance for individual membrane-bound channels. Typical PEG blockades observed using the chip were single-state (i.e. constant current) events lasting less than 1 millisecond. A high resolution view of two individual blockade events is shown in Fig. 7(b).

A current trace from a single experiment was recorded and analyzed for PEG blockade identification. Approximately 6 200 blockades were identified below the 5σ noise floor (~109.5 pA) during the detection period (500 s). The nominal open (non-occluded) channel current remained ~140 pA indicating a single α-HL channel throughout the experiment.

A histogram of blockade average currents generated from the ~6 200 blockade events is shown in Fig. 7(c). A large peak at approximately 33 pA was observed with a small peak around 100 pA. Also plotted in Fig. 7(c) are dotted lines representing the 5σ noise floor and ceiling along with the nominal open channel current of ~140 pA.

When a polydisperse PEG analyte interacts with an α-HL ion channel, higher molecular weight species produce deeper and longer blockades. This interaction causes asymmetry in the main histogram peak of the blockade average currents as summarized in Robertson and co-workers.[45] The minor peak situated around
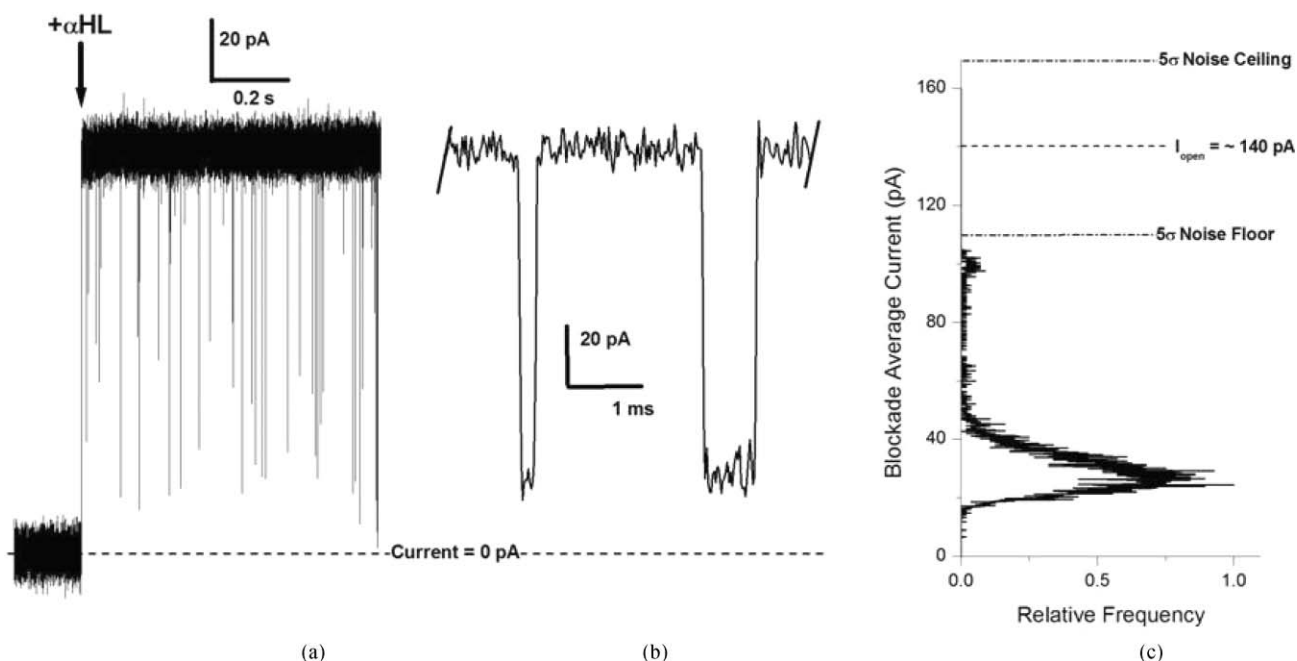
Fig. 7 (a) Current trace showing single α-HL channel incorporating with a series of PEG-1500 blockades occurring, and (b) close-up of two PEG-1500 blockades both with lifetimes on the order of half a millisecond. (c) Histogram showing relative frequency of blockade average currents generated from over 6 200 blockade events occurring below the 5σ noise floor. Data collected using a + 40 mV clamping voltage with a sampling rate of 50 kHz. All data is filtered using a 4-pole low pass Bessel filter (f_c = 10 kHz) with a background buffer of 3 M KCl and 10 mM MES (pH 7).

100 pA contains 124 of the total 6 200 blockades is attributed to α-HL channel gating chatter.

A previous study demonstrated that each size PEG in the polydisperse mixture causes blockade with a residence time distribution each described by a single exponential and that the mean residence time increases with polymer size.[45] A histogram showing the PEG residence time distribution for ~ 6 200 blockades in our system is shown in Fig. 8. Over 99% of the blockades were less than 1 ms in duration. An estimate for the aggregate residence time of all the polymers in the PEG-1500 mixture is ~ 0.12 ms.
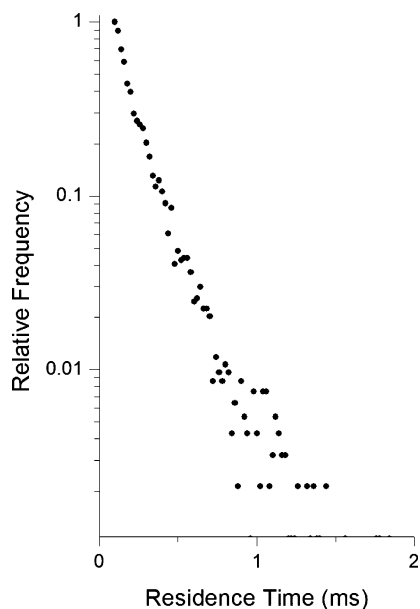
Fig. 8 Histogram showing relative frequency of ~6 200 PEG-1500 blockade lifetimes.

Conclusion

A polymer microfluidic system has been successfully applied to the detection of single PEG-1500 molecules using an individual α-HL ion channel supported within an on-chip bilayer membrane. The technology reported here represents a first step towards realizing a robust and disposable platform for performing single-molecule electrophysiology experiments, with potential benefits when compared with traditional macroscale ion channel characterization systems. Further levels of integration, including in-situ BLM formation based on our previous efforts,[46] are expected to enable improvements in system automation, and may ultimately provide a path towards a platform suitable for field-deployable single molecule biosensing.

Acknowledgements

References

1 P. Mueller, H. T. Tien, W. C. Wescott and D. O. Rudin, *Circulation*, 1962, **26**, 1167.
2 P. Mueller, D. O. Rudin, H. T. Tien and W. C. Wescott, *Nature*, 1962, **194**, 979.
3 P. Mueller, W. C. Wescott, D. O. Rudin and H. T. Tien, *Journal of Physical Chemistry*, 1963, **67**, 534–537.
4 M. Montal and P. Mueller, *PNAS*, 1972, **69**, 3561–3566.
5 A. Finkelstein, in *Methods in Enzymology*, ed. S. Fleischer, and L. Packer, Academic Press, New York, 1974, pp. 489–501.
6 S. H. White, D. C. Petersen, S. Simon and Masaoyafuso, *Biophysical Journal*, 1976, **16**, 481–489.
7 W. D. Niles, R. A. Levis and F. S. Cohen, *Biophysical Journal*, 1988, **53**, 327–335.
8 W. Hanke, and W. Schlue, *Planar Lipid Bilayers: Methods and Applications*, Academic Press, London, 1993.
9 *Ion Channel Reconstitution*, Plenum Press, New York, 1986.
10 G. Menestrina, *Journal of Membrane Biology*, 1986, **90**, 177–190.
11 W. F. Wonderlin, A. Finkel and R. J. French, *Biophysical Journal*, 1990, **58**, 289–297.
12 J. Kasianowicz and S. Bezrukov, *Biophysical J.*, 1995, **69**, 94–105.
13 M. Rhee and M. Burns, *Trends in Biotechnology*, 2006, **24**, 580–586.
14 S. Bezrukov, I. Vodyanoy, R. Brutyan and J. J. Kasianowicz, *Macromolecules*, 1996, **29**, 8517–8522.
15 R. Murphy and M. Muthukumar, *Journal of Chemical Physics*, 2007, 126.
16 V. Sharma, K. Stebe, J. C. Murphy and L. Tung, *Biophysical Journal*, 1996, **71**, 3229–3241.
17 G. C. Troiano, L. Tung, V. Sharma and K. J. Stebe, *Biophysical Journal*, 1998, **75**, 880–888.
18 N. Fertig, R. H. Blick and J. C. Behrends, *Biophysical Journal*, 2002, **82**, 3056–3062.
19 N. Fertig, C. Meyer, R. H. Blick, C. Trautmann and J. C. Behrends, *Physical Review E*, 2001, **6404**, 0901.
20 H. Suzuki, K. Tabata, Y. Kato-Yamada, H. Noji and S. Takeuchi, *Lab on a Chip*, 2004, **4**, 502–505.
21 H. Suzuki, Y. Kato-Yamada, H. Noji, and S. Takeuchi, in *Proceedings of the 17th IEEE International Conference on MEMS, Maastrict*, 2004, pp. 272–275.
22 H. Morgan, M. E. Sandison, G. Mendes, R. Berry, and A. Watts, in *8th International Conference on Miniaturized Systems for Chemistry and Life Sciences*, Malmo, Sweden, 2004, pp. 330–332.
23 H. Suzuki, K. Tabata, Y. Kato-Yamada, H. Noji and S. Takeuchi, in *8th International Conference on Miniaturized Systems for Chemistry and Life Sciences*, Malmo, Sweden, 2004, pp. 246–248.
24 H. Suzuki, K. V. Tabata, H. Noji and S. Takeuchi, *Langmuir*, 2006, **22**, 1937–1942.
25 K. Funakoshi, H. Suzuki, and S. Takeuchi, in *9th International Conference on Miniaturized Systems for Chemistry and Life Sciences*, Boston Massachusetts, 2005, pp. 951–953.
26 K. Funakoshi, H. Suzuki and S. Takeuchi, *Analytical Chemistry*, 2006.
27 M. E. Sandison, and H. Morgan, in *9th International Conference on Miniaturized Systems for Chemistry and Life Sciences*, Boston, Massachusetts, 2005, pp. 1249–1251.
28 M. E. Sandison and H. Morgan, *Journal of Micromechanics and Microengineering*, 2005, **15**, S139–S144.
29 M. R. R. de Planque, M. G. M. Zagnoni, M. E. Sandison, M. Fisher, K. Berry, A. Watts and H. Morgan, *IEE Proceedings–Nanobiotechnology*, 2006, **153**, 21–30.
30 H. Suzuki, K. Tabata, H. Noji, and S. Takeuchi, in *Proceedings of the 3rd Annual International IEEE EMBS Special Topic Conference on Microtechnologies in Medicine and Biology*, Kahuku Oahu Hawaii, 2005, pp. 272–275.
31 H. Suzuki, K. Tabata, H. Noji and S. Takeuchi, *Biosensors & Bioelectronics*, 2007, **22**, 1111–1115.

32 M. Zagnoni, M. E. Sandison, R. Wood, P. Roach, and H. Morgan, in *10th International Conference on Miniaturized Systems for Chemistry and Life Sciences*, Tokyo, Japan, 2006, pp. 1342–1344.

33 N. Malmstadt, M. Nash, R. Purnell and J. Schmidt, *Nanoletters*, 2006, **6**, 1961–1965.

34 N. Malmstadt, M. Nash, R. Purnell, and J. Schmidt, in *10th International Conference on Miniaturized Systems for Chemistry and Life Sciences*, Tokyo, Japan, 2006, pp. 1366–1368.

35 S. D. Ogier, R. J. Bushby, Y. L. Cheng, S. D. Evans, S. W. Evans, A. T. A. Jenkins, P. F. Knowles and R. E. Miles, *Langmuir*, 2000, **16**, 5696–5701.

36 Y. Cheng, R. J. Bushby, S. D. Evans, P. F. Knowles, R. E. Miles and S. D. Ogier, *Langmuir*, 2001, **17**, 1240–1242.

37 S. J. Wilk, L. Petrossian, M. Goryll, T. J. Thornton, S. M. Goodnick, J. M. Tang and R. S. Eisenberg, *Biosensors and Bioelectronics*, 2007, **23**, 183–190.

38 M. E. Sandison, M. Zagnoni and H. Morgan, *Langmuir*, 2007, **23**, 8277–8284.

39 M. Zagnoni, M. E. Sandison, P. Marius, A. G. Lee and H. Morgan, *Lab Chip*, 2007, **7**, 1176–1183.

40 J. A. Maurer, V. E. White, D. A. Dougherty and J. L. Nadeau, *Biosensors and Bioelectronics*, 2007, **22**, 2577–2584.

41 R. Sherman-Gold, *Axon Instruments*, 1993.

42 B. J. Polk, A. Stelzenmuller, G. Mijares, W. MacCrehan and M. Gaitan, *Sensors and Actuators B-Chemical*, 2006, **114**, 239–247.

43 M. Misakian and J. J. Kasianowicz, *Journal of Membrane Biology*, 2003, **195**, 137–146.

44 A. Aksimentiev and K. Schulten, *Biophysical Journal*, 2005, **88**, 3745–3761.

45 J. Robertson, C. Rodrigues, V. Stanford, K. Rubinson, O. Krasilnikov and J. J. Kasianowicz, *Proceedings of the National Academy of Sciences of the United States of America*, 2007, **104**, 8207–8211.

46 L. Hromada, J. Kasianowicz, M. Gaitan, D. Millard, and D. L. DeVoe, *10th International Conference on Miniaturized Systems for Chemistry and Life Sciences*, 2006, 531–533.